

Identification of Mosquito Larvae through Image- Processing and Object Detection Using Machine Learning Algorithms

Naviya Gupta

Dhirubhai Ambani International School Mumbai, India
naviyagupta@outlook.com

Reetu Jain

Founder and Mentor,
On My Own Technology Pvt Ltd reetu.jain@onmyowntechnology.com

Abstract— In urban areas based in tropical latitudes, mosquito vectors pose an immense risk to human health and the quality of life. For years, the mitigation of lethal, vector borne diseases such as malaria, dengue and chikungunya has been sought through the application of localised insecticides for the elimination of adult mosquitoes. However, growing congestion and overpopulation presents the need to prevent the spread of vector-borne diseases at the source itself. The prototype which is the focus of this paper, the Smart Mosquito Larvae Detector, consists of a 3D printed, hollow cylindrical body, a camera attachment, Styrofoam supports to aid floatation, a set of batteries for electrical input and a microprocessor. This state-of-the-art model utilises image processing algorithms under Single-shot Transfer learning. Implementing object detection frameworks from an expansive dataset of larvae images, the proposed methodology aims to detect viable mosquito larvae in stagnant water bodies or containers, and subsequently notifying authorities of the presence of these vector larvae in order to mitigate their spread.

Keywords—Mosquito larvae, Image Processing, Convolutional Neural Networks, Malaria

I. INTRODUCTION

Ever since Sir Ronald Ross' ground-breaking

discovery in 1897, identifying the female Anopheles mosquito as the vector responsible for the transmission of malaria via carriage of the Plasmodium species of parasite [1], mosquitoes have been dubbed the world's deadliest animal. Mosquito-borne diseases such as malaria, dengue, yellow fever, chikungunya and the Zika virus are responsible for up to 7,00,000 annual deaths, and 500,00,000 annual cases (UN World Health Organization, 2020). These diseases abound in the tropical and subtropical regions of the world, their adverse effects appearing most prominently in economically poorer nations with underdeveloped health infrastructure and an uncontrollably expanding population [2].

Statistics obtained from the World Health Organization's database show that the three cardinal pathogen-carrying mosquito species include Anopheles, Aedes and Culex. The female Anopheles species, whose disease carrying properties are attributed as the discovery of Sir Ross, is the vector for the transmission of malaria, naturally abounding in southeast Asia, including the Asia-Pacific region. Although malaria poses the greatest threat to the region of Sub-Saharan Africa, which accounts for 93% of malaria cases and 94% of deaths worldwide (World Health Organization, 2018), the Indian subcontinent is another epicentre for the disease, with its impact in India accounting for 52% of global malaria-related deaths outside sub-Saharan Africa and 1.2% of malaria deaths worldwide (World Malaria Report, 2021). Conversely, the Aedes species transmits the diseases dengue, yellow fever, zika virus and

chikungunya. This, in turn, leads to 50 million annual cases and 300,000 annual deaths in tropical and sub-tropical latitudes [3]. The Culex mosquito has the widest species-wise distribution globally, present in all latitudes except for the northern temperate areas. It aids the spread of diseases such as West Nile virus, St. Louis encephalitis and Japanese encephalitis (Centres for Disease Control and Prevention, 2009; World Health Organization, 1997), and can be established as one of the chief vectors and carriers of disease-causing microbes and pathogens in the Indian subcontinent [4].

| Year | Point | Number of cases (000) | | | % P. vivax | Point | Number of deaths | | |
|------|---------|-----------------------|-------------|------|------------|---------|------------------|-------------|--|
| | | Lower bound | Upper bound | | | | Lower bound | Upper bound | |
| 2000 | 207 000 | 192 000 | 223 000 | 2.0% | 840 000 | 813 000 | 871 000 | | |
| 2001 | 212 000 | 196 000 | 230 000 | 2.1% | 838 000 | 809 000 | 873 000 | | |
| 2002 | 209 000 | 193 000 | 227 000 | 1.8% | 797 000 | 770 000 | 832 000 | | |
| 2003 | 211 000 | 195 000 | 231 000 | 1.9% | 774 000 | 744 000 | 819 000 | | |
| 2004 | 212 000 | 194 000 | 239 000 | 1.7% | 750 000 | 718 000 | 818 000 | | |
| 2005 | 209 000 | 192 000 | 232 000 | 1.1% | 723 000 | 696 000 | 772 000 | | |
| 2006 | 209 000 | 191 000 | 232 000 | 1.2% | 715 000 | 686 000 | 761 000 | | |
| 2007 | 209 000 | 191 000 | 230 000 | 1.2% | 698 000 | 670 000 | 741 000 | | |
| 2008 | 209 000 | 192 000 | 228 000 | 1.0% | 678 000 | 652 000 | 715 000 | | |
| 2009 | 212 000 | 194 000 | 234 000 | 1.2% | 671 000 | 640 000 | 723 000 | | |
| 2010 | 212 000 | 194 000 | 235 000 | 1.5% | 646 000 | 613 000 | 702 000 | | |
| 2011 | 209 000 | 193 000 | 230 000 | 2.1% | 608 000 | 579 000 | 652 000 | | |
| 2012 | 209 000 | 192 000 | 228 000 | 2.4% | 575 000 | 544 000 | 620 000 | | |
| 2013 | 207 000 | 191 000 | 227 000 | 2.2% | 566 000 | 523 000 | 602 000 | | |
| 2014 | 204 000 | 187 000 | 223 000 | 2.2% | 534 000 | 503 000 | 561 000 | | |
| 2015 | 204 000 | 187 000 | 223 000 | 1.7% | 527 000 | 496 000 | 577 000 | | |
| 2016 | 209 000 | 189 000 | 224 000 | 1.1% | 528 000 | 497 000 | 582 000 | | |
| 2017 | 213 000 | 196 000 | 233 000 | 0.8% | 542 000 | 510 000 | 607 000 | | |
| 2018 | 211 000 | 194 000 | 232 000 | 0.7% | 533 000 | 500 000 | 605 000 | | |
| 2019 | 212 000 | 194 000 | 233 000 | 0.3% | 534 000 | 498 000 | 616 000 | | |
| 2020 | 228 000 | 206 000 | 266 000 | 0.3% | 602 000 | 560 000 | 738 000 | | |

Figure 1: Number of malaria cases and deaths from 2000- 2020 as estimated by the WHO - World Malaria Report, 2021 (Image credit)

Total Percentage of Global Malaria-Related Deaths

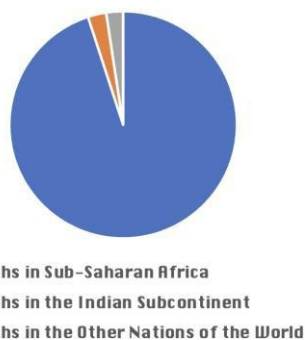


Figure 2: Graphical View of Malaria-Related Deaths Worldwide (%)

Mosquitoes thrive in bodies of stagnant water, often in water-carrying containers such as buckets, tubs, fountains, artificial ponds and puddles after rain, all widely available in urban areas [5]. The adult female mosquito lays her eggs on the walls of the stagnant vessel or on the surface of the still water. The life cycle of a mosquito consists of three stages after the laying of eggs: the larvae, the pupa and

finally, the adult mosquito [6]. A female mosquito can lay as many as 100 eggs at a time to maximise survival of their offspring, and after the water completely submerges the eggs, viable larvae emerge from the eggs. These larvae obtain nourishment from microbes in the water and gradually form a pupal skin, from which winged adult mosquitoes emerge in 2-3 days [7].

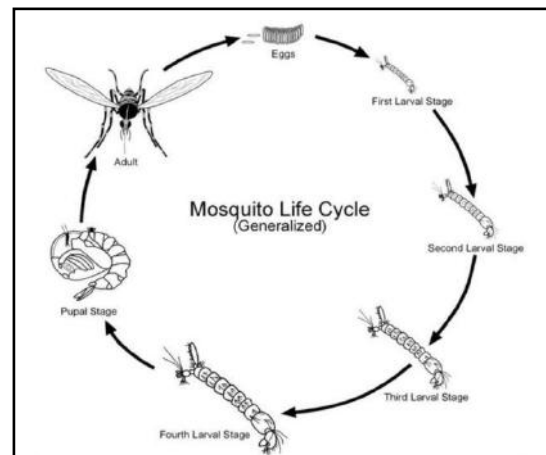


Figure 3: The Life Cycle of a Mosquito (Image credits)

In the present day, the solution to the nuisance of mosquitoes and the diseases they bear presents itself in the form of adulticides, i.e., methodologies used to exterminate active adult mosquitoes. These include chemical compounds and insecticides such as organophosphates and synthetic pyrethroids, as well as aerosols, insect electrocutors and ultra-low volume (ULV) spray applicators [8][9]. However, while these methods can eliminate mosquito pests in small numbers, they are less effective in mitigating the spread of these vectors. Hence, due to the localised nature of how mosquito eggs are laid, and their immense quantity, it would be more effective to mobilise their elimination by targeted means, i.e., mobilising a mechanism to detect viable mosquito larvae, hatched from eggs, in stagnant water containers and bodies [10].

II. LITERATURE REVIEW

Existing research towards the prevention and mitigation of vector-borne diseases includes a wide range of solutions for identification of breeding mosquitoes and their eggs, and their subsequent extermination through chemical or mechanical means (predominantly through the use of high frequency sound) [11] [12].

A majority of these methodologies focus on the

detection of mosquitoes in the larval stage, making use of machine learning and artificial intelligence. Deep learning, a branch of machine learning modelled after the layered neural processing network of the human brain, is a particularly prevalent computational model applied to the recognition and identification or classification of mosquito larvae from a dataset of images [13][14]. For classification and recognition of mosquito larvae in images of stagnant water from the dataset, the use of Convolutional Neural Networks (CNN) has proven to be particularly effective [15], including methods such as ImageNet, for visual object recognition research [16].

However, these methodologies often involve the usage of costly equipment for the procurement of a sample, such as optic lenses, laboratory slides and smartphone storage [17]. Additionally, a large portion of research has been dedicated towards deep learning and image classification architectures devoted to classification of detected larvae into specific species [18] [19] and cannot be directly deployed into stagnant water bodies, resulting in expenditure of time in collection of a sample from such breeding grounds.

The more conducive solutions seek to construct a working hardware system that can be deployed in stagnant water containers [20], and make use of image processing [21] or segmentation techniques [22] through CNN architectures, detecting presence of larval activity.

III. MOTIVATION AND NOVELTIES

Through a machine-learning based image processing methodology, this paper aims to optimise mitigation of the spread of vector-borne diseases such as dengue and malaria by targeting the root of the vector itself, mosquito larvae, for effective extermination. Although there has been adequate exploration and technological review of adult vector- extermination, there is great potential for more effective elimination through larvae detection in stagnant water samples, before they develop into viable adult disease- carrying vectors. Further, the lack of technological mechanisms in the vector detection process results in manual identification being the predominant approach, resulting in local officials becoming increasingly susceptible to infection in the name of public

health. Thus, the existence of this prototype as a compact body conducive to floatation allows for it to be deployed in stagnant water bodies and to minimise health risks to officials from manual inspection.

IV. METHODOLOGY

The Smart Mosquito Larvae Detector's working mechanism relies on image processing through the Single-Shot Transfer learning model. Input as images of the stagnant water surface captured by the floating device are processed by object detection algorithms, run against the annotated dataset of mosquito larvae used to train the model, and finally the user is notified of the density of larvae detected in the images collected by the device's inbuilt camera with high accuracy. Thus, the device can be directly deployed in stagnant water to detect varying densities of larval breeding.

The hardware of the device consists of a 3D printed hollow disc shape (14 cm in diameter), Styrofoam supports to facilitate buoyancy, a Raspberry Pi Zero Camera Module to capture live feed of the water samples, interfaced with the RaspberryPi processor. The input from the camera is processed against the object detection algorithms, and used to identify individual larvae and their proximity, thus alerting authorities of the presence of potential.

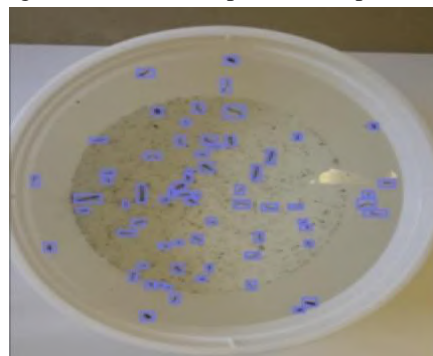


Figure 4: Annotated image with low larval density

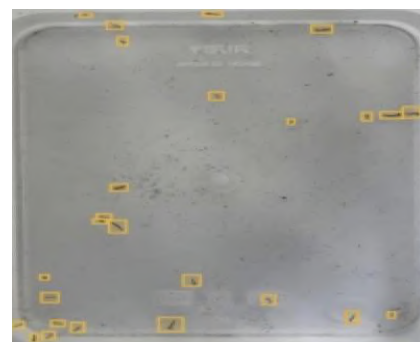


Figure 5: Annotated image with high larval density

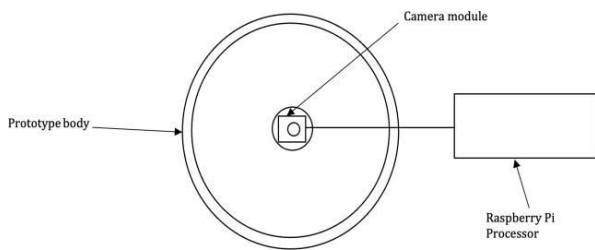


Figure 6A: Diagrammatic overhead view of prototype

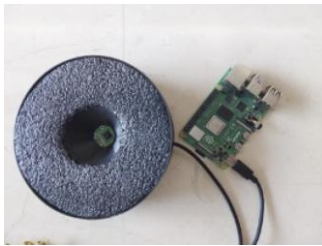


Figure 6B: Actual view of prototype

A. Data Collection

The meticulous dataset utilised for this research consists of images taken of a sample of mosquito larvae in a container holding stagnant water kept over a period of 30 days. The sample consisted of both *Aedes* and *Anopheles* mosquito larvae at various stages of development in their life cycle. A tripod stand with an iPhone camera was utilised in order to take 2-minute-long, overhead video captures of the sample. Subsequently, images were extracted from this set of videos for image annotation necessary for object detection algorithms to be applied to the dataset. These images were taken following a pattern to maintain consistency of the dataset: 4 times in a 24-hour span with 4-hour intervals, taken daily at 7 am, 11 am, 3 pm and 7 pm.



Figure 7A: Image taken at 7 am



Figure 7B: Image taken at 11 am



Figure 7C: Image taken at 3 pm



Figure 7D: Image taken at 7 pm

B. Data Pre-Processing

Before the dataset of images could be implemented

into the pre-trained algorithm, there was extensive data pre-processing. The purpose of image pre-

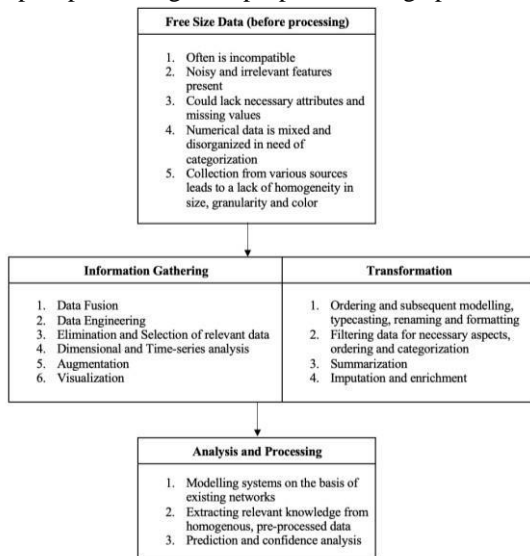


Figure 8: Tabular flowchart depicting data pre-processing requisites and function ([Image Credit](#))

processing in transfer learning is to ensure the highest image quality to maximise the efficiency and accuracy of results. This includes the elimination of any distortions and enhancement of features that are conducive to the application, allowing the image files to be converted into floating-point tensors for input into the framework. Pre-processing producers often consist of colour adjustments, size homogeneity (256x256 pixels) and ensuring uniform orientation across the dataset. Uniformity of size and orientation is imperative in neural network models, as it is a requirement due to the layers' complete connectivity that the images for processing are in identically sized arrays.

Before training the model for this device, the image annotations were ascertained to be in the correct orientation to train the machine-learning structures in accordance with the user's physical view of the images (EXIF data depicting how the system stores the images in relation to its input orientation). As the dataset consisted of differently sized images, images were resized in order to ensure ease of conversion to arrays- as the jpg file format was converted to NumPy arrays for each image to allow processing. Further, to ensure a uniform signal was imparted to all the "neurons" of this AI-based system, a colour transformation was applied to the image files, with the default RGB colour profile of the images captured on an iPhone camera being converted into a BGR scheme for OpenCV. Other

than the assurance of uniformity, this step was taken to ensure that the OpenCV (cv2) library (which has restrictions on the colour profile of images utilised) accepts the files to be converted to arrays.

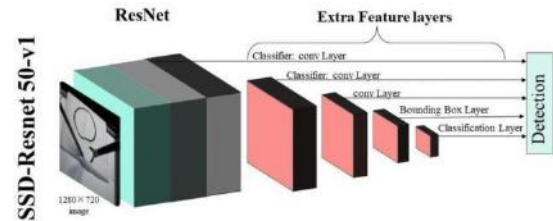


Figure 9: SSD ResNet50 Model Architecture ([Image credits](#))

7. Object Detection

This methodology uses single-shot Transfer learning algorithms based on pre-trained models for object detection of the larvae in images of the water sample. Due to the collected dataset consisting of 100 images, there came the need to employ a state-of-the-art pre-trained model by transferring and adapting the pre-learned features of the model to the new dataset. For this algorithm, the SSD ResNet50 model was utilized, a deep convolutional network model with 50 layers of processing. The most significant feature of this model is its ability to skip connections during training, mitigating a "vanishing gradient" in deeper convolutional layers. In this case, transfer learning is utilized for feature extraction from the dataset collected, wherein convolutional and pooling layers identify progressively complex patterns, features and descriptive elements within the data provided by the user. An image from the dataset is taken as the input, and the weights already assigned to features in the pre-trained model were used to classify a new dataset inputted by the user (in this case, the mosquito larvae), rendering them distinct in the algorithm. As the input image progresses through the initial layers and residual blocks (characteristic of this model), basic visual elements such as patterns, textures and shapes are identified, while skipping connections to provide more complex enhancement and refinement of the features extracted. Venturing into the deeper levels, the model begins to draw associations between features and objects in the input images, generating feature maps at every stage to depict the object detections in various regions of the image. The analysis

becomes more attuned to the inputted dataset, and employs modification and classification of pre-trained model in this respect.

This model was created on TensorFlow using a sequential structure and its architecture is based on the pre-trained Single-Shot Detector ResNet50 model. Training the model involved the use of 100 out of 175 annotated images in the dataset, with the remaining 75 utilised for verification of the methodology. In data pre-processing, there were size adjustments to each of the images to ensure uniformity so that the input images have homogenous colours and dimensions, i.e., 224x224 pixels, RGB dataset. The architecture of the model also includes the skipping of 3 layers by the shortcut connections, depicted below:

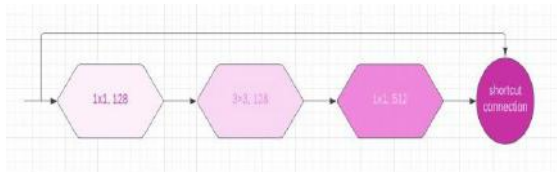


Figure 10: Skipping 3 connections to prevent “vanishing gradient”

After the image is inputted into the model, the annotated mosquito larvae objects are extracted via the laying of kernels (or learnable filters) on the input image. As the input data ventured deeper into the network layers, the number of filters increased in number and complexity, allowing more sophisticated detection of larvae. After each layer, non-linearity was re-introduced to the model to allow the capture of variations and complex patterns. This is achieved via the Rectified Linear Unit (ReLU) or the non-linear activation function, which reassigns values to negative pixels, replacing them with zero. While increasing the complexity of analysis, the computational complexity was also managed to retain the efficiency of the transfer learning model: pooling layers reduced the spatial dimensions of larval maps while retaining all the necessary data obtained. The penultimate step before the data began its passage through the fully connected layers involved the flattening of larval maps from the pooling layers into a one-dimensional vector, to allow effectiveness of further processing.

Finally, the activation feature associates the model’s predictions on the feature map with a probability score between 0 and 1, representing the

model’s confidence in the presence of mosquito larvae in the sample. The minimum confidence threshold for the model utilised for this device is set to 0.5, and only larvae with a probability score greater than 0.5 will be displayed as detection. Further, the code uses visualisation to depict detection of larvae, with class labels laid on the input images with bounding boxes and confidence scores for detected objects.

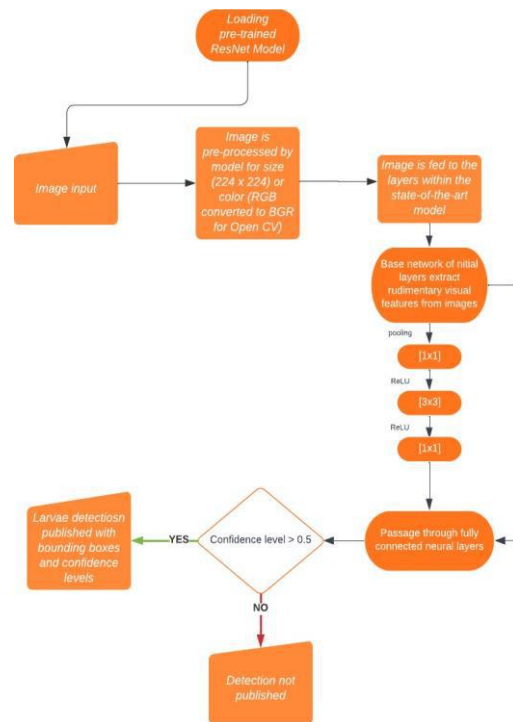


Figure 11: Flowchart depicting the working of the Object Detection Algorithm using a SSD ResNet50 (pre-trained state-of-the-art model)

V. PROTOTYPE AND DESIGN

A. Electronic Components

The prototype consisted of a 3D-printed, cylindrical disk-like body (14 cm diameter) as well as electronic hardware such as a Raspberry Pi Zero Camera Module with a wired connection to the Raspberry Pi processor. The prototype has an intended function of floatation, to allow deployment in water bodies, where images will be captured of the water surface via the camera module every 2 minutes, allowing live detection of mosquito larvae. Thus, to avoid damage from aquatic exposure, the electronic components are all covered with a protective, watertight casing. A single wired connection emerging from a hole on the top of the lid controls the distance travelled by

the prototype, and holds it steady for effective image capture in stagnant water.

B. 3D Design

In order to ensure buoyancy of the device, a lightweight material would have to be employed for construction of the disk body. Thus, 3D printing was utilised with a filament of Polyethylene Terephthalate Glycol (PETG) for mechanical strength as well as functionality of prototype. Referring to Archimedes' fundamental principle of floatation, buoyancy would only be possible if the average density of the device was lower than that of water. Thus, multiple CAD designs underwent testing and rejection in order to arrive at the model that possessed the required average density and did not capsize when loaded with electrical components such as the Raspberry Pi processor and the camera module.

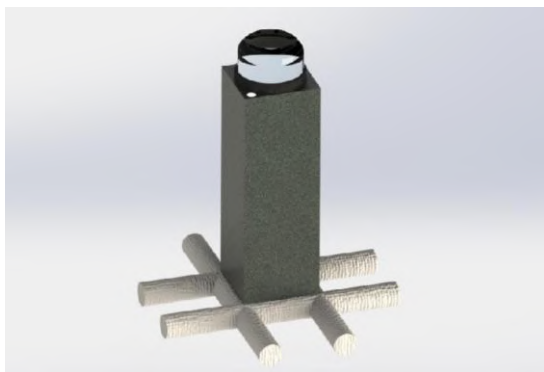


Figure 12: Preliminary CAD design with towering projection

The initial design possessed a tower-like projection with the camera fitted on top of it and a hollow cavity ending in a hole at the raft-like apparatus forming the base. This was to allow adequate distance of the camera from the water surface to avoid damage. However, the towering projection also increased the height of the centre of gravity of the device thus resulting in it toppling easily. Subsequently, modifications were implemented in the CAD design of the prototype, arriving at a disk-like cylindrical shape with a height of 5 cm, lowering the centre of gravity and allowing a compact design.

A vertical conical hole was designed to be emerging from the base (widest at the bottom, and tapering

with height) to allow the camera to have maximum range of capture.

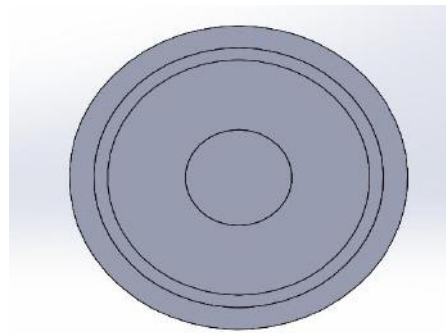


Figure 13A: Top view of first model (with raft)
Further, two scaled-down, test prototypes were printed. The first had a hollow cavity around a solid projection with a raft underneath for support. The second had a hollow cavity around a solid projection with a thin border and no raft. The hollow spaces would be stuffed with a foam filling to allow for a lower average density. When tested for floatation, it was found that a surrounding hollow cavity was better suited to bearing weight and maintained more stability on the water surface. Thus, the second design was printed to scale and implemented with the remaining hardware.

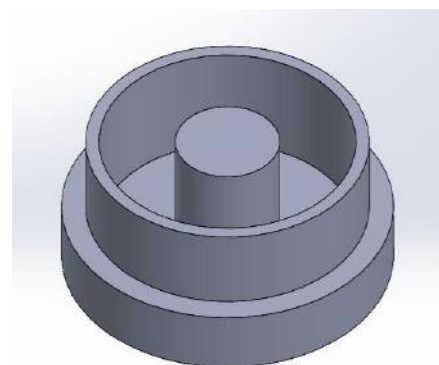


Figure 13B: Isometric view of first model (with raft)

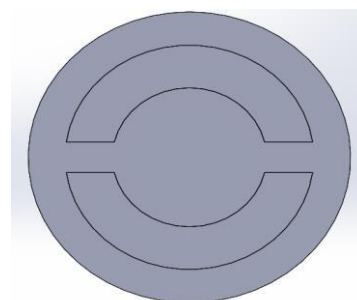


Figure 14A: Top view of second model (without raft)

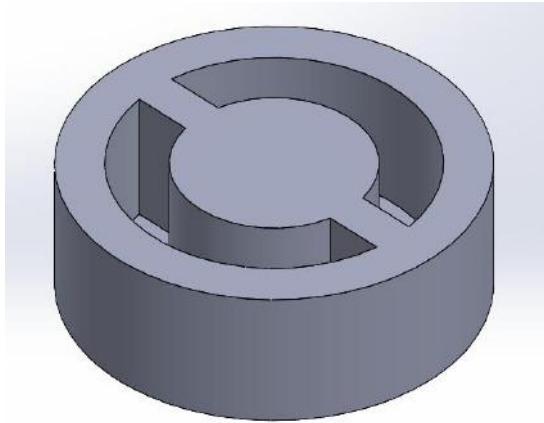


Figure 14B: Isometric view of second model (without raft)



Figure 15: Top View of final 3D printed prototype (to scale) hollow cavities stuffed with foam

VI. OBSERVATIONS AND RESULTS

The created model was run on a macOS Monterey (12.5) processor through a VNC viewer. The Raspberry Pi processor was connected via an HDMI cable, and the data recorded from the images captured every 2 minutes was stored in the computer display's system. The holistic functionality of the prototype's hardware and software was tested by the device's receptiveness to images of a singular mosquito larva, low density and high density, as well as a real stagnant water surface. The Single-Shot Transfer model network was trained on 50 free size images of high larval

density as well as 50 free size images of low larval density taken at different points in the day to allow adjustments for lighting and colour. (to scale) hollow cavities stuffed with foam

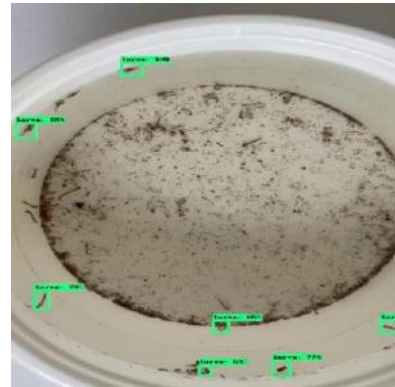


Figure 16: Test data depicting larval detections with respective bounding boxes and confidence levels

It was found through testing that the overall accuracy rate of the algorithm is 95%. Time series were obtained using the following code, which gave an overview of the system's testing, including loss and learning rates:

```
%reload_ext tensorboard  
%tensorboard --logdir  
"/content/gdrive/MyDrive/Larvae_Detection /data  
for  
larvae_Detection/models/my_ssd_resnet101_v1_fpn"
```

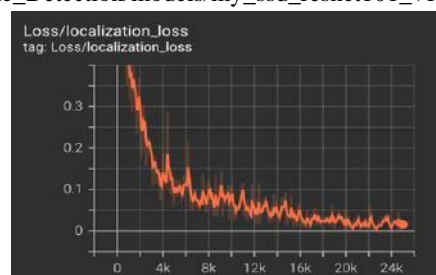


Figure 17A: Classification loss with respect to checkpoints

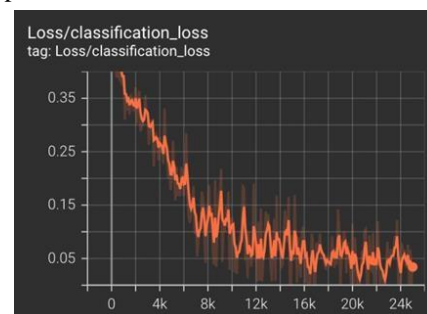


Figure 17B: Localization loss with respect to checkpoints

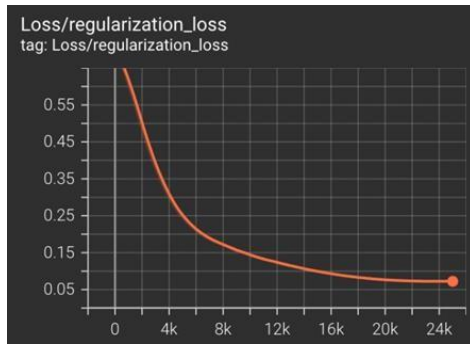


Figure 17C: Regularization loss with respect to checkpoints

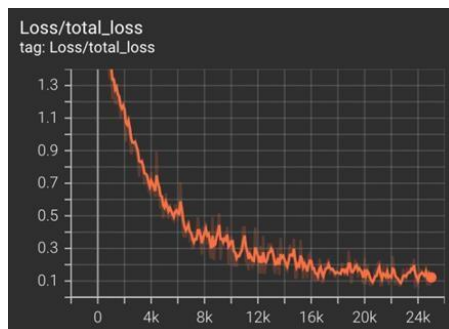


Figure 17D: Total loss with respect to checkpoints

The data displayed above indicates the process of training the model and the trends in loss as well as the steps taken through 25,000 checkpoints during its implementation.

The input images below visually depict the passage of input data through various steps engaging in increasingly complex analysis:

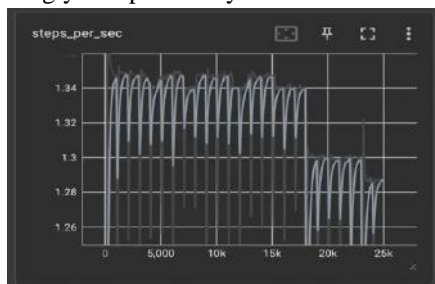


Figure 18: Steps per second in training the model with respect to checkpoints 0 to 25000

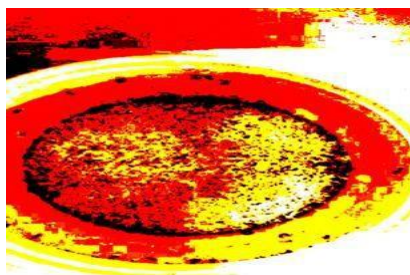


Figure 19A: Trained input image at step 24,000

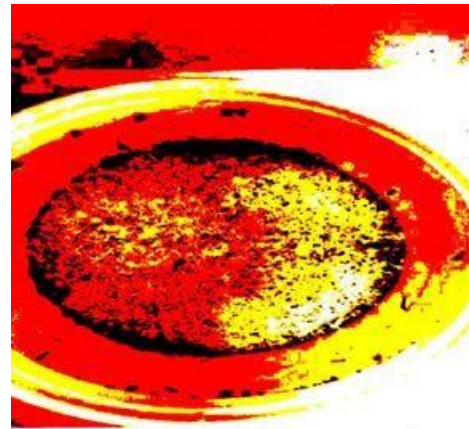


Figure 19B: Trained input image at step 24,500

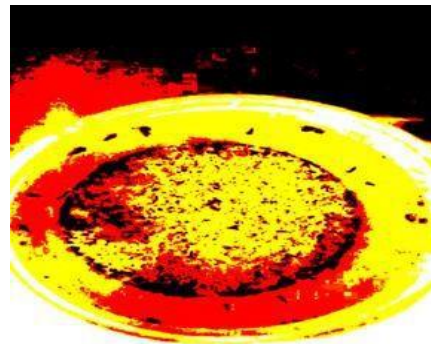


Figure 19C: Trained input image at step 24,900

The image quality affects detection, as a low pixel count results in an unclear shape and borders of the larvae, thus resulting in a lower confidence reading. Since the confidence threshold for this model lies at 0.5, only detections with a higher probability reading are displayed, resulting in better accuracy.

The data procured from testing shows that the accuracy of detection in this device is of a sufficiently high level. A wider dataset of images, as well as a higher quality of image could result in greater accuracy of detection, providing future scope of improvement for this prototype.

VII. CONCLUSION AND DISCUSSION

There is a great volume of existing research on the detection of mosquito eggs via image segmentation, or the extermination of adult vectors. However, detection at the egg stage cannot account for the number of viable vectors, and adult extermination can only serve as a localised solution, and cannot mitigate the spread of disease carrying vectors. Thus, this research provides for an

effective tool that addresses the problem of spread of viable vectors at their very root, targeting mosquito larvae.

Thus, in order to achieve the outlined objectives, a floating prototype consisting of a disk-like 3D printed body, a camera module and a Raspberry Pi processor was built with the intended use of it being deployed in stagnant water bodies or containers to allow for image capture and subsequent detection of mosquito larvae present in the water sample. The device yields a high accuracy of detection (95%), which allows for effective detection of mosquito larvae in both high and low density. The device and algorithm also consist of a number of useful features such as the prototype's lightweight nature and capacity for floatation, as well as immediate capture of images in a minimal time interval (2 minutes). Additionally, the generation of bounding boxes and class labels on detection allow for easy analysis of the presence of larvae and observation of the positions and dimensions of individual larvae detected.

Although the accuracy of detection by this device is high, future scope of improvement includes using a greater and more expansive dataset of images with different capture angles and lighting to increase accuracy. Further, the glare of artificial or natural light on a water surface could disrupt image capture, but this could be easily rectified by providing a flat underwater or surface bounding to the area of capture below the device, minimising light exposure and allowing high-quality image capture.

To conclude, this compact and easy-to-use device allows for non-manual and accurate detection of mosquito larvae, which not only aids in early detection and mitigation of the spread of mosquito-borne diseases, but also eliminates the need for manual inspection of stagnant water bodies, thus greatly reducing the exposure of municipal authorities to these highly contagious vector-borne diseases.

REFERENCES

1. Sinden RE. Malaria, mosquitoes and the legacy of Ronald Ross. *Bull World Health Organ.* 2007 Nov;85(11):894-6. doi: 10.2471/blt.04.020735. PMID: 18038083; PMCID: PMC2636258.
2. Knudsen AB, Slooff R. Vector-borne disease problems in rapid urbanization: new approaches to vector control. *Bull World Health Organ.* 1992;70(1):1-6. PMID: 1568273; PMCID: PMC2393336
3. Mubbashir H, Munir S, Kashif R, Nawaz HB, Abdul B, Baharullah K. Characterization of dengue virus in *Aedes aegypti* and *Aedes albopictus* spp. of mosquitoes: A study in Khyber Pakhtunkhwa, Pakistan. *Mol Biol Res Commun.* 2018 Jun;7(2):77-82. doi: 10.22099/mbrc.2018.29073.1315. PMID: 30046621; PMCID: PMC6054776.
4. Sharma, Ajay & Mendki, Mj & Tikar, Sachin & Kulkarni, Girish & Veer, Vijay & Prakash, Shri & Shouche, Yogesh & Parashar, B.D.. (2010). Molecular phylogenetic study of *Culex quinquefasciatus* mosquito from different geographical regions of India using 16S rRNA gene sequences. *Acta tropica.* 116. 89-94. 10.1016/j.actatropica.2010.06.003.
5. Haroon, Atif, et al. "Water resources helps in the expansion of mosquitoes colonies." *Big Data In Water Resources Engineering (BDWRE)* 1.1 (2020): 16-21.
6. Kalman, Bobbie. *The life cycle of a mosquito.* Crabtree Publishing Company, 2004.
7. Jayakumar, M., T. Samuel, and S. John William. "Aedes: An ever dangerous enemy to our society." *Defeating the public enemy, the mosquito: A real challenge,* Loyola publications, Chennai, Tamil Nadu, India (2007): 205-221.
8. Bonds, J. A. S. "Ultra-low-volume space sprays in mosquito control: a critical review." *Medical and veterinary entomology* 26.2 (2012): 121- 130.
9. Baitharu, Iswar, et al. "Environmental Management and Sustainable Control of Mosquito Vector: Challenges and Opportunities." *Molecular Identification of Mosquito Vectors and Their Management* (2020): 129-147.
10. M. S. Saeed, S. F. Nazreen, S. S. S. A. Ullah, Z. F. Rinku and M. A. Rahman, "Detection of Mosquito Larvae Using Convolutional Neural Network," 2021 2nd International Conference on Robotics, Electrical and Signal Processing Techniques (ICREST), DHAKA, Bangladesh, 2021, pp. 478-482, doi: 10.1109/ICREST51555.2021.9331235.
11. C. A. B. Mello, W. P. dos Santos, M. A. B. Rodrigues, A. L. B. Candeias and C. M. G. Gusmao, "Image segmentation of ovitraps for automatic counting of *Aedes Aegypti* eggs," 2008 30th Annual International Conference of the IEEE Engineering in Medicine and Biology Society,

- Vancouver, BC, Canada, 2008, pp. 3103-3106, doi: 10.1109/IEMBS.2008.4649860.
12. Kalimuthu K, Tseng L-C, Murugan K, Panneerselvam C, Aziz AT, Benelli G, Hwang J-S. Ultrasonic Technology Applied against Mosquito Larvae. *Applied Sciences*. 2020; 10(10):3546. <https://doi.org/10.3390/app10103546>
 13. Y. LeCun, Y. Bengio, and G.E. Hinton. (2015). "Deep Learning." *Nature* Volume 521, 436–444.
 14. Asmai, Siti & Abas, Zuraida & Mohamad Jaya, Abdul. (2019). Mosquito Larvae Detection using Deep Learning. *International Journal of Innovative Technology and Exploring Engineering*. 8. 804-809. 10.35940/ijitee.L3213.1081219.
 15. M. S. Saeed, S. F. Nazreen, S. S. S. A. Ullah, Z. F. Rinku and M. A. Rahman, "," 2021 2nd International Conference on Robotics, Electrical and Signal Processing Techniques (ICREST), DHAKA, Bangladesh, 2021, pp. 478-482, doi: 10.1109/ICREST51555.2021.9331235.
 16. O. Russakovsky, J. Deng, H. Su, J. Krause, S. Satheesh, S. Ma, Z.H. Huang, A. Karpathy, A. Khosla, M. Bernstein, A.C. Berg and L. Fei- Fei. (2014). "ImageNet Large Scale Visual Recognition Challenge." *arXiv preprint arXiv:1409.0575*. Accessed on May 2019 from <https://arxiv.org/abs/1409.0575>
 17. M. I. A. B. Z. Azman and A. B. Sarlan, "Aedes Larvae Classification and Detection (ALCD) System by Using Deep Learning," 2020 International Conference on Computational Intelligence (ICCI), Bandar Seri Iskandar, Malaysia, 2020, pp. 179-184, doi: 10.1109/ICCI51257.2020.9247647.
 18. García, Zaira & Yanai, Keiji & Nakano, Mariko & Arista, Antonio & Cleofas, Laura & Perez-Meana, Hector. (2019). Mosquito Larvae Image Classification Based on DenseNet and Guided Grad-CAM. 10.1007/978-3-030-31321-0_21.
 19. Akter, Mehenika & Hossain, Mohammad & Ahmed, Tawsin & Andersson, Karl. (2021). Mosquito Classification Using Convolutional Neural Network with Data Augmentation. 10.1007/978-3-030-68154- 8_74.
 20. Amruth V, et. al. "Mosquito Larvae Detection and Killing System." *International Journal of Advances in Engineering and Management (IJAEM)*, 2(1), 2020, pp. 357-361. DOI: 10.35629/5252-45122323
 21. Surya, Aswin & Peral, David & VanLoon, Austin & Rajesh, Akhila. (2022). A Mosquito is Worth 16x16 Larvae: Evaluation of Deep Learning Architectures for Mosquito Larvae Classification. 10.48550/arXiv.2209.07718.
 22. Fuad, M.A., Ghani, M.R., Ghazali, R., Izzuddin, T.A., Sulaima, M.F., Jano, Z., & Sutikno, T. (2019). Detection of Aedes aegypti larvae using single shot multibox detector with transfer learning. *Bulletin of Electrical Engineering and Informatics*.

FIGURES

1. Figure 1: Mosquito trapping in Recreational Parks of Selangor and their role in Public Health - Scientific Figure on ResearchGate
2. Figure 3: Rogozi, Elton. (2010). Mosquito trapping in Recreational Parks of Selangor and their role in Public Health. 10.13140/2.1.4697.7608.
3. Figure 7: Asmai, Siti & Abas, Zuraida & Mohamad Jaya, Abdul. (2019). Mosquito Larvae Detection using Deep Learning. *International Journal of Innovative Technology and Exploring Engineering*. 8. 804-809. 10.35940/ijitee.L3213.1081219.
4. Figure 8: Box-Trainer Assessment System with Real- Time Multi-Class Detection and Tracking of Laparoscopic Instruments, using CNN Box-Trainer Assessment System with Real-Time Multi-Class Detection and Tracking of Laparoscopic Instruments, using CNN - Scientific Figure on ResearchGate Available from: https://www.researchgate.net/figure/SSD-ResNet50-V1-FPN-Architecture_fig2_356909958 [accessed 11 Sep, 2023]
5. Figure 9: Multistage Model for Robust Face Alignment Using Deep Neural Networks - Scientific Figure on ResearchGate Available from: https://www.researchgate.net/figure/Structure-of-a-residual-unit_fig4_349875225 [accessed 11 Sep, 2023]